JOC The Journal of Organic Chemistry

Article

pubs.acs.org/joc

Palladium-Mediated Catalysis Leads to Intramolecular Narcissistic Self-Sorting on a Cavitand Platform

Zoltán Nagymihály,[†] Naidel A. M. S. Caturello,[‡] Anikó Takátsy,[§] Gemma Aragay,[∥] László Kollár,[†] Rodrigo Q. Albuquerque,[‡,⊥] and Zsolt Csók*[,‡]

[†]Department of Inorganic Chemistry and MTA-PTE Research Group for Selective Chemical Syntheses, University of Pécs, Ifjúság 6, 7624 Pécs, Hungary

[‡]São Carlos Institute of Chemistry, University of São Paulo, Av. Trab. São-carlense 400, 13560-970 São Carlos, SP, Brazil

[§]Department of Biochemistry and Medical Chemistry, Medical School, University of Pécs, Szigeti 12, 7624 Pécs, Hungary

[∥]Institute of Chemical Research of Catalonia (ICIQ), Av. Països Catalans 16, 43007 Tarragona, Spain

[⊥]School of Pharmacy & Biomolecular Sciences, Liverpool John Moores University, Liverpool L3 3AF, United Kingdom

Supporting Information

ABSTRACT: Palladium-catalyzed aminocarbonylation reactions have been used to directly convert a tetraiodocavitand intermediate into the corresponding carboxamides and 2-ketocarboxamides. When complex mixtures of the amine reactants are employed in competition experiments using polar solvents, such as DMF, no "mixed" products possessing structurally different amide fragments are detected either by ^{1}H or ^{13}C NMR. Only highly symmetrical cavitands are sorted out of a large number of potentially feasible products, which represents a rare example of intramolecular, narcissistic self-sorting. Our experimental results along with thermodynamic energy analysis suggest that the observed self-sorting is a symmetry-driven, kinetically controlled process.

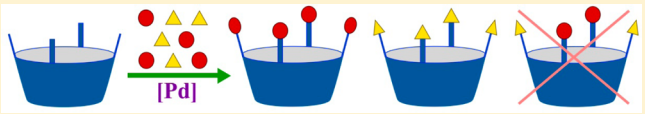

INTRODUCTION

Molecular self-sorting represents the ability to distinguish "self" from "non-self" within complex mixtures.[1] In recent years, the rapid evolution of supramolecular chemistry brought the phenomenon of self-sorting into the limelight.[2,3] Self-sorting plays a crucial role in the construction of intricate molecular architectures in complex biological systems.[4] The most prominent example for molecular self-sorting is perhaps the formation of the DNA double helix, which requires orthogonal base-pairing of nitrogen-containing nucleobases through intermolecular hydrogen bonds between the two separate polynucleotide strands (adenine-thymine and cytosine-guanine).[5] By definition, narcissistic self-sorting occurs between the same species (self-recognition), whereas social self-sorting arises between different species (self-discrimination).[1] Recently, Schalley et al. introduced the term integrative self-sorting, in which all elements in a multicomponent library selectively self-sort into one single complex assembly.[6,7]

The overwhelming majority of self-sorting occurs between single molecular components, which are usually driven by various classes of noncovalent interactions. Complementary hydrogen bonding is the most commonly used structural motif for the construction of intermolecularly self-sorted (and self-assembled) multimeric systems. Efficient and clean self-sorting of modified calix[4]arenes or cavitands, that are capable of making hydrogen bonding, led to the spontaneous formation of well-defined, artificial self-assemblies.[8−13] Metal coordination was also found useful for achieving high fidelity self-sorting of various cavitand ligands, which resulted in the selective self-assembly of coordination cages in competition experiments.[14−16] Furthermore, it was shown that the extent of self-sorting greatly depends on the guest size during the formation of water-soluble dimeric capsules driven by the hydrophobic effect.[17] However, to the best of our knowledge, only two studies have been recently reported on intramolecular self-sorting, which involved dynamic covalent chemistry in the syntheses of various peptido-cavitands.[18,19]

Carboxamidocavitands, obtained usually by the acylation of the corresponding aminocavitands,[20,21] have strong tendency to form self-assembled dimeric capsules via intermolecular hydrogen bonds.[22] In contrast, we used palladium-catalyzed carbonylative amidation (or aminocarbonylation) reactions to directly convert a versatile tetraiodocavitand intermediate[23] into the corresponding tetra(carboxamido)- and tetra(2-ketocarboxamido)cavitands.[24,25] Interestingly, very high chemoselectivities have been observed toward these tetrafunctionalized cavitands as 1) no substantial formation of either mono-, di- or trifunctionalized products was obtained, and 2) no "mixed" products possessing both carboxamide and 2-ketocarboxamide fragments were detected. Based on these observations, we wondered whether competition experiments between two or more amines as N-nucleophiles in palladium-catalyzed carbonylation reactions would produce such high selectivities. For this reason, we designed and synthesized novel tetra(carboxamido)-cavitands as reference compounds, and performed palladium-

Received: October 10, 2016
Published: December 16, 2016

DOI: 10.1021/acs.joc.6b02472
J. Org. Chem. 2017, 82, 390−396

Scheme 1. 4-fold Palladium-Catalyzed Carbonylative Amidation of Tetra(iodo)cavitand[a]

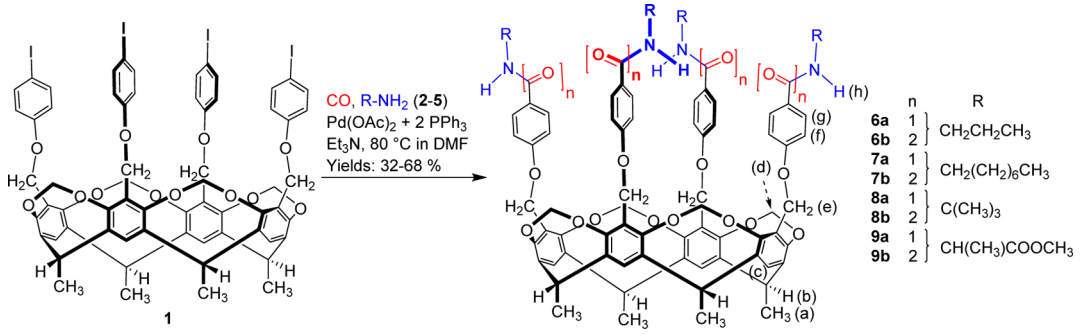

[a]Proton designations are in parentheses.

mediated catalytic self-sorting experiments using up to four different amine reactants in various complex mixtures. Quantum chemical calculations at the semiempirical PM6 level were also used to gain insight on the thermodynamic versus kinetic reaction pathways.

RESULTS AND DISCUSSION

Palladium-Catalyzed Carbonylative Amidation. In 4-fold palladium-catalyzed aminocarbonylation, tetraiodocavitand (**1**) was reacted with *n*-propylamine (**2**) (or *n*-octylamine (**3**) or *t*-butylamine (**4**) or D-alanine methyl ester hydrochloride (**5**)) in the presence of an *in situ* palladium catalyst ($Pd(OAc)_2$ + 2 PPh_3) and Et_3N base under atmospheric carbon monoxide pressure at 80 °C for 48 h (Scheme 1). The role of the $Pd(OAc)_2$ precursor and two equiv of PPh_3, acting as both ligand and reducing agent, is to form coordinative highly unsaturated and reactive Pd(0) catalyst species. The oxidative addition step of the aminocarbonylation reaction requires Pd(0) species, which can be obtained via reduction by using PPh_3 as reducing agent. While one of the two triphenylphosphines is oxidized to $P(O)Ph_3$, and consequently Pd(II) is reduced to Pd(0), the "second" PPh_3 is coordinated to the Pd(0) species to form a highly reactive catalytic intermediate. The NEt_3 base, acting as hydrogen iodide acceptor, is necessary to complete the full catalytic cycle of the aminocarbonylation reaction.

All reactions led to the simultaneous formations of the corresponding tetra(carboxamido)- (**6a**–**9a**) and tetrakis(2-ketocarboxamido)cavitands (**6b**–**9b**) by single (n = 1) or double (n = 2) carbon monoxide insertion, respectively (Table 1, run 1–8), and were fully characterized by traditional methods. ^1H–^1H COSY techniques were used to establish atom connectivities and exact peak assignments (for proton designations, see Scheme 1). Being away from the reaction centers, the ^1H NMR chemical shifts of the H_a–H_e protons in the cavitand skeleton are almost identical in all amide derivatives. In contrast, the ^1H NMR signals of the H_f–H_h protons can be used as diagnostic tools for the determination of the product compositions, as these resonances appear at different chemical shifts in the two differently carbonylated products (Supporting Information, Table S1). Particularly, the ^1H chemical shifts of the amide N–H protons (H_h) of compounds **6b**–**9b** show significant downfield shifts in the range of 0.52–0.87 ppm when compared to those of **6a**–**9a**.

In full accordance with the refs 24 and 25, no substantial formation of "mixed" products possessing both carboxamide and 2-ketocarboxamide fragments were observed. A slight excess of the amine reactants (5 mol equiv with respect to **1**) resulted in the preferential formation of **6a**–**9a**. Furthermore, we have also noticed that the mol equiv of Et_3N base to iodoarene functionalities (Et_3N/substrate ratio) have an influence on the product composition: the lower the Et_3N/substrate ratio, the higher the ratio of **6a**–**9a** to **6b**–**9b** in the product mixtures. That is, the formation of **6a**–**9a** is favored by using 2 mol equiv of triethylamine instead of 20 mol equiv. In spite of the potential fine-tuning of the reaction conditions, most of these carboxamides were accompanied by 2-ketocarboxamides in these atmospheric carbonylation reactions (Table 1, run 2, 4, and 6). Due to the very similar physicochemical properties of the mono- and the double-carbonylated derivatives, we failed to isolate compounds **6a**–**9a** in acceptable purities by column chromatography in carbonylative amidation reactions.

Higher CO pressure (60 bar) and large excess (20 mol equiv with respect to **1**) of the amine reactants (as well as the Et_3N base) afforded predominantly **6b**–**9b** (Table 1, run 9–12), as reported elsewhere for similar reactions,[24,25] however, compound **6b** could only be identified in a mixture with **6a**. The formation of the novel double-carbonylated cavitands (**6b** and **7b**) was unequivocally confirmed by MALDI-TOF and by the appearance of an additional downfield carbonyl peak around 189 ppm in their ^{13}C NMR spectra (Supporting Information, Figure S5 and S11).

Table 1. Product Compositions in Palladium-Catalyzed Aminocarbonylations of Tetraiodocavitand[a]

run	amine	mol equiv of amine	p[CO] (bar)	mol equiv of Et_3N	product composition[b] (%)
1	**2**	5	1	20	15 (**6a**)/85 (**6b**)
2	**2**	5	1	2	80 (**6a**)/20 (**6b**)
3	**3**	5	1	20	35 (**7a**)/65 (**7b**)
4	**3**	5	1	2	85 (**7a**)/15 (**7b**)
5	**4**	5	1	20	45 (**8a**)/55 (**8b**)
6	**4**	5	1	2	65 (**8a**)/35 (**8b**)
7	**5**	5	1	20	85 (**9a**)/15 (**9b**)
8	**5**	5	1	2	> 95 (**9a**)
9	**2**	20	60	20	15 (**6a**)/85 (**6b**)
10	**3**	20	60	20	> 95 (**7b**)
11	**4**	20	60	20	> 95 (**8b**)
12	**5**	20	60	20	> 95 (**9b**)

[a]Reaction conditions: **1**/$Pd(OAc)_2$/PPh_3 = 1:0.15:0.3; 80 °C, 48 h. [b]Determined on the crude reaction mixture by the integration of the corresponding ^1H NMR peaks, as indicated in Table S1 in the Supporting Information.

DOI: 10.1021/acs.joc.6b02472
J. Org. Chem. 2017, 82, 390–396

Synthesis of the Reference Compounds. Full interpretation of molecular self-sorting experiments, in which numerous products may form with almost identical characteristics, requires reliable characterization of sufficiently pure reference compounds. Therefore, we looked for an alternative reaction pathway to access pure carboxamidocavitands before embarking on self-sorting studies. Carboxamide fragments were successfully introduced into similar cavitand scaffolds by amination of the corresponding acyl chlorides.[26,27] Following this strategy, cavitands **6a**–**9a** were readily synthesized in one-pot reactions from a recently reported tetra(carboxyl)cavitand (**10**)[28] (Scheme 2). First, cavitand **10** was reacted with thionyl chloride in the presence of catalytic amount of DMF to afford the corresponding tetrakis(acyl-chloride)cavitand. Then, the *in situ* treatment of this nonisolated intermediate with the required amines (**2**–**5**) gave pure **6a**–**9a** in good yields (39–58%). The ^{1}H NMR spectra of these compounds in $CDCl_3$ exhibited broad signals, which is indicative of the formation of ill-defined aggregates in this solvent. On the contrary, the ^{1}H NMR spectra of **6a**–**9a** displayed well-resolved, sharp proton signals in DMSO-d_6, a competitive solvent that can disrupt hydrogen bonds, and were consistent with C_4 symmetries (Figure 1a–d).

Scheme 2. Synthesis of Tetra(carboxamido)cavitands as Reference Compounds

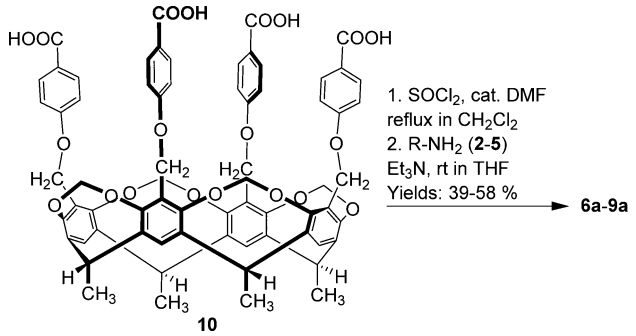

Palladium-Catalyzed Self-Sorting Experiments. Palladium-catalyzed carbonylation reactions, including all possible binary amine combinations, were performed in the presence of 2 mol equiv of Et_3N base under atmospheric carbon monoxide pressure using DMF as solvent (Table 2, run 1–6).

Table 2. Product Compositions in Pd-Catalyzed Self-Sorting Experiments Using DMF as Solvent[a]

run	mixture of amines	product composition[b] (%)
1	**2**/**3**	40 (**6a**)/60 (**7a**)
2	**2**/**4**	92 (**6a**)/8 (**8a**)
3	**2**/**5**	80 (**6a**)/20 (**9a**)
4	**3**/**4**	60 (**7a**)/8 (**8a**)
		32 (**7b**)
5	**3**/**5**	75 (**7a**)/25 (**9a**)
6	**4**/**5**	35 (**8a**)/65 (**9a**)
7	**2**/**3**/**4**/**5**	47 (**6a**)/32 (**7a**)
		5 (**8a**)/1 (**9a**)
		15 (**6b**/**7b**)

[a]Reaction conditions: **1**/Et_3N/$Pd(OAc)_2$/PPh_3 = 1/2/0.15/0.3; *p*[CO] = 1 bar, 80 °C, 48 h. The ratio of the amines was kept identical in the mixtures: 5 mol equiv each with respect to **1**. [b]Determined on the crude reaction mixture by the integration of the corresponding ^{1}H NMR signals (Figure 1).

Accordingly, two-component amine mixtures of **2**/**3**, **2**/**4**, **2**/**5**, **3**/**4**, **3**/**5**, and **4**/**5** (5 mol equiv each) were reacted with tetraiodocavitand (**1**) in these competition experiments. Statistically, a two-component mixture can combine to form six different products on a macrocyclic platform possessing four reaction sites (Figure 2). Remarkably, the ^{1}H and ^{13}C NMR

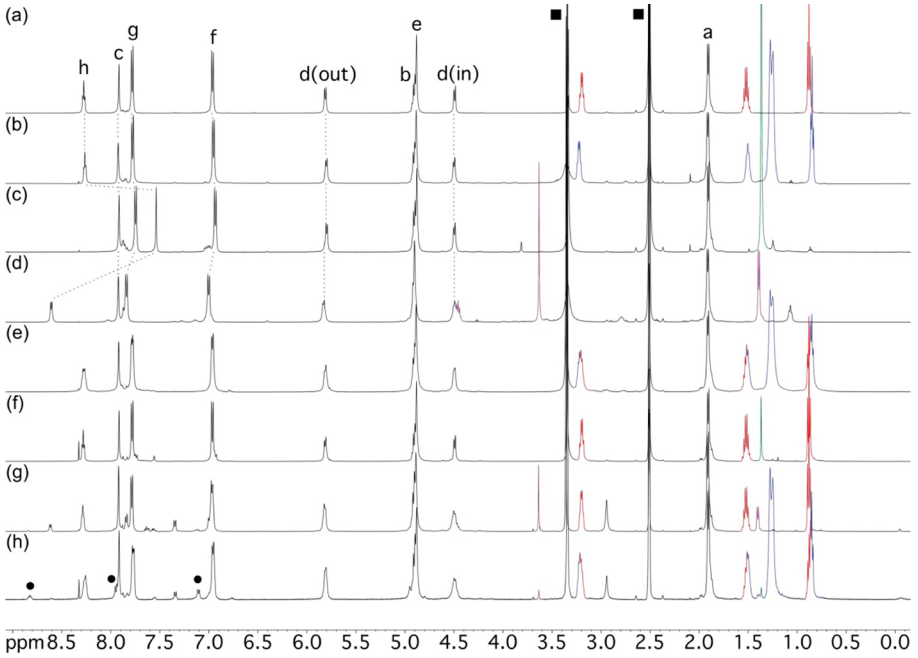

Figure 1. ^{1}H NMR spectra (500 MHz, DMSO-d_6, 25 °C) of reference compounds (a) **6a**, (b) **7a**, (c) **8a**, (d) **9a**, and those of the products obtained in Pd-catalyzed self-sorting experiments involving mixtures of amines (e) **2**/**3**, (f) **2**/**4**, (g) **2**/**5**, and (h) **2**/**3**/**4**/**5** (● denotes double-carbonylated products (**6b** and **7b**), whereas ■ stands for the residual signals of DMSO-d_6 and HDO).

DOI: 10.1021/acs.joc.6b02472
J. Org. Chem. 2017, 82, 390–396

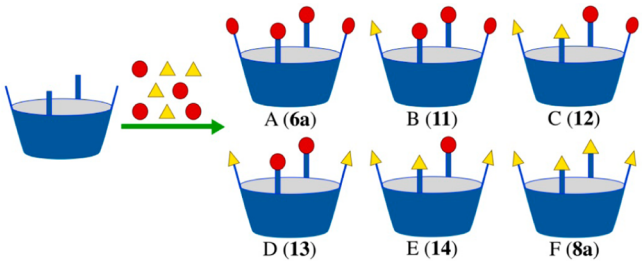

Figure 2. Statistical combinations of a two-component reactant mixture on a macrocyclic platform possessing four reaction sites (species A–F).

spectra of the products obtained in the carbonylation reactions involving these amine mixtures are the exact pairwise superpositions of those of the corresponding pure tetra(carboxamido)cavitands (Figure 1e–g and Figure S21–S26 in the Supporting Information). It is important to note that the ^{13}C resonances of the major products of these competition experiments are very sharp, and strictly reproduce the corresponding chemical shifts of the "nonmixed" reference compounds by at least one decimal place. If "mixed" carboxamidocavitands possessing two structurally different amide fragments (and thus having less symmetrical structures) were formed, both the ^{1}H and the ^{13}C NMR spectra would be much more complicated. Nevertheless, the presence of "mixed" compounds (<5%), as a result of imperfect self-sorting, cannot be completely ruled out, and some minor NMR peaks can be attributed to these products. Curiously, in contrast to the "nonscrambled" experiments described earlier, no formation of double-carbonylated cavitands was observed in any of these trials, with the exception of run 4, which afforded 32% of 2-ketocarboxamide **7b**. Therefore, out of six possible combinations, this intramolecular self-sorting typically ended up in two highly symmetrical products. To quantitatively differentiate between various sorting processes, Schmittel et al. defined the degree of self-sorting as $M = P_0/P$, where P_0 is the number of all possible combinations, whereas P is the number of all observed species in the experiment.[3] Accordingly, $M = 3$ was calculated for all of these intramolecular self-sorting processes.

The direct comparison of the product distributions in these two-component competition experiments allowed us to study the different reactivities of the amine reactants on this cavitand platform. The mixture of **2**/**3** gave rise to **6a** and **7a** in almost equal quantities (Table 2, run 1), whereas the scrambling of **2** with either **4** or **5** afforded predominantly **6a** (Table 2, run 2, 3). Likewise, the mixing of **3** with either **4** or **5** provided essentially **7a**, along with smaller quantities of **8a** and **9a** (Table 2, run 4, 5). Finally, the competition experiment between **4** and **5** resulted in the formation of 35% of **8a** and 65% of **9a** (Table 2, run 6). On these grounds, a clear reactivity order of the four amine reagents can be defined: **2** (*n*-propylamine) ≈ **3** (*n*-octylamine) > **5** (D-alanine methyl ester hydrochloride) > **4** (*t*-butylamine).

Next, we investigated the sorting of all four possible amine components (**2**/**3**/**4**/**5**, 5 eq. each) in one single competition experiment (Table 2, run 7). Taking into account redundancies arising from symmetry considerations, a quaternary mixture can statistically bring about 49 different products when combined on a four-branched macrocyclic skeleton. Again, the highly symmetrical ^{1}H and ^{13}C NMR spectra proved the simultaneous formation of "nonmixed" carboxamidocavitands (**6a**/**7a**/**8a**/**9a**), and the integration of the corresponding NMR peaks indicated that **6a** and **7a** were the main components (Figure 1h and Figure S27, S28 in the Supporting Information). It has to be noted that about 15% of double-carbonylated products (**6b** and **7b**) could also be identified among the products, but we could not perform more precise quantitative NMR analysis due to excessive peak overlaps. Nevertheless, it can be stated that only four symmetrical "nonmixed" carboxamide compounds are sorted out of a large numbers of potentially possible products ($M = 12.25$) taking into account monocarbonylation. This trial also confirmed the established reactivity order of the amine reactants obtained in the binary scrambling experiments, that is, **2** ≈ **3** > **5** > **4**.

We have also studied the effect of different solvents on the product distribution of these Pd-catalyzed aminocarbonylation reactions. Using THF as solvent, the product composition of the competition experiment involving the mixture of **2**/**3** was comparable to the one obtained in DMF. Interestingly, when toluene was used as solvent, additional peaks emerged in both the ^{1}H and ^{13}C NMR spectra of the product (Figure S29 and S30 in the Supporting Information). Appearing very close to the known chemical shifts of the reference compounds **6a** and **7a**, the new resonances of these amide alkyl protons can be attributed to "mixed" cavitand species. Nevertheless, cavitands **6a** and **7a** proved to be the main products (~80%) also in this experiment. Accordingly, the high-fidelity self-sorting occurring in polar reaction media (DMF, THF) turns into less obvious in the less polar toluene.

Molecular Modeling. Self-sorting systems generally proceed along thermodynamic pathways, however, kinetic controls of self-sorting are also known.[29−31] In a thermodynamically controlled self-sorting, the products reach a thermodynamic equilibrium corresponding to the lowest overall Gibbs energy. On the other hand, in a kinetically controlled process, the products can be regarded as trapped species under kinetic control that correspond to the lowest activation energies. By means of molecular modeling, we attempted to determine which reaction pathway (thermodynamic or kinetic) plays a decisive role in the final composition of the products in these self-sorting experiments. It has to be noted, however, that performing solid reaction kinetics of palladium-catalyzed carbonylations would be a formidable task on this relatively sizable cavitand platform. Therefore, we essentially aimed to obtain reliable thermodynamic data for the formation of both "pure" and "mixed" products.

Semiempirical calculations using the PM6 model[32] were carried out in vacuum for the "pure" **6a**–**9a**, and also for a full set of "mixed" compounds **11**–**14**, decorated with various combinations of *n*-propyl and *t*-butyl groups. According to Figure 2, exclusive *n*-propyl substitution represents **6a** (species A), while a full "*t*-butyl swap" gives **8a** (species F). If one of the *n*-propyl groups in **6a** is replaced by a *t*-butyl, cavitand **11** is obtained (Figure 2, species B). Cavitands **12** and **13**, bearing two *n*-propyl and two *t*-butyl moieties, are structural isomers, in which the same amido groups are situated at 1,2- or 1,3-positions, respectively (Figure 2, species C and D). Finally, the conversion of three *n*-propyl groups in **6a** into *t*-butyl fragments affords cavitand **14** (Figure 2, species E). In another series of semiempirical calculations, the solvent effect was considered by the application of the COSMO model, which uses an implicit solvent layer represented by a continuous dielectric medium.[33] In addition to the geometry optimizations, the enthalpies and the entropies were also computed for these molecules, relative

DOI: 10.1021/acs.joc.6b02472
J. Org. Chem. 2017, 82, 390−396

to the elements in their standard state at 298 K both in vacuum and in DMF solvent (COSMO model), as shown in the Supporting Information (Tables S2 and S3). The energy-minimized structures of the tetra(carboxamido)cavitands **6a** and **8a** are shown in Figure 3.

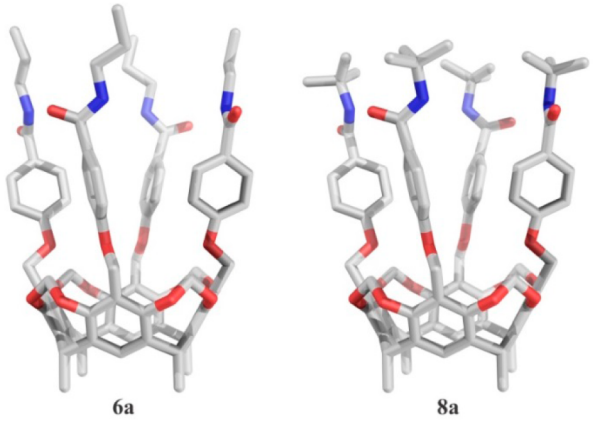

Figure 3. Energy-minimized structures of tetra(carboxamido)cavitands **6a** and **8a** using the semiempirical PM6 model in DMF (COSMO) at 298 K. Hydrogens are omitted for clarity.

The variations in the Gibbs energies ($\Delta_f G$) associated with the formation of these carboxamidocavitands (eq 1) were calculated according to eqs 2–4):

$$\text{cavitand}(\mathbf{1}) + 4\cdot\text{CO} + n\cdot\mathbf{2} + (4-n)\cdot\mathbf{4} \rightarrow \text{carboxamidocavitand} + 4\cdot\text{HI} \quad (1)$$

$$\Delta_f G = \Delta_f H - T\cdot\Delta_f S \quad (2)$$

$$\Delta_f H = \Delta H_{(\text{amidocavitand})} + 4\cdot\Delta H_{(\text{HI})} - \Delta H_{(\mathbf{1})} - 4\cdot\Delta H_{(\text{CO})} - n\cdot\Delta H_{(\mathbf{2})} - (4-n)\cdot\Delta H_{(\mathbf{4})} \quad (3)$$

$$\Delta_f S = \Delta S_{(\text{amidocavitand})} + 4\cdot\Delta S_{(\text{HI})} - \Delta S_{(\mathbf{1})} - 4\cdot\Delta S_{(\text{CO})} - n\cdot\Delta S_{(\mathbf{2})} - (4-n)\cdot\Delta S_{(\mathbf{4})} \quad (4)$$

where the quantities of $\Delta H_{(x)}$ and $\Delta S_{(x)}$ were calculated relative to the elements in their standard state. The changes in the Gibbs energies for the carbonylation reactions affording "pure" (**6a**, **8a**) and "mixed" (**11**–**14**) products are shown in Figure 4 (see also Table S4). These values reveal that the highest negative changes in the Gibbs energies belong to the formation of **8a** and to those of the "mixed" compounds (**11**–**14**). In contrast, **6a** was predominantly formed in the competition experiment involving the mixture of **2** and **4**, and no "mixed" products were experimentally detected (Table 2, run 2). Consequently, this energy analysis proposes that these Pd-mediated carbonylations supposedly do not proceed along thermodynamic pathways. In addition, the reactivity order of the amines, established in the competition experiments, corresponds to the steric hindrance around the carbon directly attached to the NH_2 group: **2** ≈ **3** (primary carbon) > **5** (secondary carbon) > **4** (tertiary carbon). Steric crowding is well-known for decreasing reaction rates by increasing the activation energies of most chemical reactions.[34] Therefore, the reactivity order of the amine reactants and the energy analysis obtained from the semiempirical PM6 model suggest that kinetic control is one of the factors that drives this self-sorting

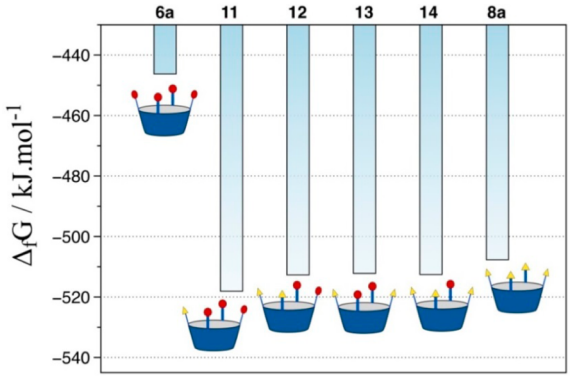

Figure 4. Changes in the Gibbs energies for the carbonylation reactions shown in (eq 1) using the semiempirical PM6 model in DMF (COSMO model) at 298 K. Red circles and yellow triangles represent *n*-propyl and *t*-butyl groups, respectively.

phenomenon. Additionally, it seems that the aryl-iodide moieties on this cavitand skeleton do not react independently, however, the exact origin of this cooperativity effect remains unclear.

CONCLUSION

In sum, 4-fold palladium-catalyzed carbonylative amination gave direct access to cavitands featuring one and two carbonyl groups in their amide functionalities along the upper rim. Amination of the corresponding tetra(acyl-chloride)cavitand led to pure carboxamidocavitands (**6a**–**9a**), which were used as reference compounds in subsequent scrambling experiments. The competition experiments involving equimolar binary and quaternary mixtures of the amine reactants in Pd-catalyzed carbonylation reactions typically ended up in the exclusive formation of the "pure" carboxamidocavitands using polar solvents, such as DMF. No "mixed" products possessing structurally different amide fragments were detected either by ^{1}H or ^{13}C NMR. Therefore, only highly symmetrical carboxamide compounds are sorted out of a large number of potentially possible products, which leads to novel selectivities in palladium-mediated catalysis. The observed symmetry-driven self-sorting is presumably credited to kinetic control, as suggested by competition experiments and by thermodynamic analysis obtained from the semiempirical PM6 model. Further experimental and computational studies involving other (catalyst-free) organic reactions are underway in our laboratories to gain a deeper understanding on the mechanistic aspects of these intriguing chemical processes.

EXPERIMENTAL SECTION

General Experimental Methods. Palladium(II) acetate (98%) was purchased from Sigma-Aldrich, and used without further purifications. The synthesis of tetra(carboxyl)cavitand (**10**) has been described in ref 28. ^{1}H and ^{13}C NMR spectra were recorded at 500 and 125 MHz, respectively. The NMR chemical shifts (δ), reported in parts per million (ppm) downfield, are referenced to the residual signals of DMSO-d_6 (2.50 ppm for ^{1}H and 39.51 ppm for ^{13}C NMR spectra, respectively). Mass spectra were obtained by MALDI-TOF using 2,5-dihydroxybenzoic acid (DHB) as matrix. Full characterization of compounds **8b** and **9b** has been previously reported.[24]

Computational Studies. The geometries of **6a**–**9a** and **11**–**14** were fully optimized by performing semiempirical calculations using the PM6 model,[32] as implemented in the MOPAC2012 program suite.[35] The solvent effect was also considered in the semiempirical calculations by the application of the COSMO model.[33] Vibrational

DOI: 10.1021/acs.joc.6b02472
J. Org. Chem. 2017, 82, 390−396

frequencies were calculated to check the reliability of the geometry optimizations by the absence of negative frequencies. The enthalpies and entropies were calculated relative to the elements in their standard state. The enthalpy values at 298 K were directly obtained from the output of the MOPAC program in the geometry optimization step. For the entropies at 298 K, thermodynamic calculations based on the molecular partition function were carried out using the same program via the keyword "thermo".

General Procedure for the Aminocarbonylation Experiments. Tetraiodocavitand (**1**) (250 mg, 0.164 mmol), $Pd(OAc)_2$ (5.6 mg, 0.025 mmol), and PPh_3 (13.1 mg, 0.05 mmol) were weighed and placed under an inert atmosphere into a 100 mL 3-necked Schlenk tube (or into a 100 mL autoclave for high pressure experiments). Dry DMF (20 mL), 0.82 mmol of the corresponding amine (**2**-**5**), and finally, 46 μL of Et_3N were added to the reaction vessel. The reaction mixture was then placed under 1 bar (or 60 bar) CO pressure, and stirred at 80 °C for 48 h. The precipitate that separated was filtered, and the filtrate was evaporated to dryness. The residue was treated with MeOH (5 mL), the resulting precipitate was collected by filtration, and thereafter dried under vacuum.

Self-Sorting Pd-Catalyzed Aminocarbonylation Experiments. The same procedure was followed. The mixture of the corresponding amines (see Table 2) was prepared in DMF (5 mL), and then this mixture was added to the reaction vessel to ensure full competition.

Synthesis of the Reference Compounds (6a−9a). Tetra(carboxyl)cavitand (**10**) (250 mg, 0.21 mmol) was dissolved in dry CH_2Cl_2 (10 mL), to which thionyl chloride (1.0 mL, 13.8 mmol) and catalytic amount of DMF (5 μL) was added under argon atmosphere. The reaction mixture was then heated to reflux under argon for 16 h. The mixture was cooled to rt, the solvent was evaporated to dryness, and the tetra(acyl-chloride)cavitand intermediate was then dissolved in dry THF (10 mL). The reaction vessel and its contents were cooled to 0 °C before the addition of 1.05 mmol of the corresponding amine (**2**−**5**) and dry Et_3N (100 μL) under argon atmosphere. The reaction mixture was stirred at rt for 24 h, the precipitate that separated was filtered, and the filtrate was evaporated to dryness. The residue was triturated with MeOH (5 mL), the resulting precipitate was collected by filtration and dried in vacuo.

Cavitand ***6a***. White solid, 58% (165 mg). mp. 181−184 °C. Anal. Calcd for $C_{80}H_{84}N_4O_{16}$: C, 70.78; H, 6.24; N, 4.13. Found: C, 71.09; H, 6.26, N, 4.11. ^{1}H NMR (500 MHz, DMSO-d_6): δ 0.87 (t, J = 7.3 Hz, 12H, CH_2CH_3), 1.51 (sext, J = 7.3 Hz, 8H, $CH_2CH_2CH_3$), 1.90 (d, J = 7.4 Hz, 12H, CH_3CH), 3.19 (q, J = 6.7 Hz, 8H, NH−CH_2CH_2), 4.48 (d, J = 7.6 Hz, 4H, inner of OCH_2O), 4.85−4.94 (br s, 12H, $ArCH_2O$ overlapping with CH_3CH), 5.80 (d, J = 7.6 Hz, 4H, outer of OCH_2O), 6.95 (d, J = 8.8 Hz, 8H, Ar), 7.77 (d, J = 8.8 Hz, 8H, Ar), 7.91 (s, 4H, Ar), 8.27 (t, J = 5.6 Hz, 4H, N−H). ^{13}C {^{1}H} NMR (125 MHz, DMSO-d_6): δ 11.4, 16.0, 22.4, 31.2, 40.9, 60.4, 99.3, 113.9, 122.40, 122.43, 127.3, 128.9, 139.0, 153.0, 160.4, 165.5 (ArC═O). IR (KBr): ν (cm^{-1}) 970, 1239, 1499, 1606, 1634, 2964. MALDI-TOF m/z: 1379.52 $[M+Na]^+$, 1357.51 $[M+H]^+$.

Cavitand ***6b***. (Identified in a mixture: **6b**/**6a** = 85/15.) Pale yellow solid, 65% (157 mg). mp. 172−177 °C. ^{1}H NMR (500 MHz, DMSO-d_6): δ 0.88 (t, J = 7.3 Hz, 12H, CH_2CH_3), 1.51 (sext, J = 7.3 Hz, 8H, $CH_2CH_2CH_3$), 1.90 (d, J = 7.3 Hz, 12H, CH_3CH), 3.18 (q, J = 6.6 Hz, 8H, NH−CH_2CH_2), 4.47 (d, J = 7.4 Hz, 4H, inner of OCH_2O), 4.85−4.98 (br s, 12H, $ArCH_2O$ overlapping with CH_3CH), 5.82 (d, J = 7.4 Hz, 4H, outer of OCH_2O), 7.09 (d, J = 8.8 Hz, 8H, Ar), 7.92 (s, 4H, Ar), 7.94 (d, J = 8.8 Hz, 8H, Ar), 8.80 (t, J = 5.9 Hz, 4H, N−H). ^{13}C {^{1}H} NMR (125 MHz, DMSO-d_6): δ 11.3, 16.0, 22.0, 31.3, 40.1, 60.7, 99.4, 114.7, 122.0, 122.6, 126.0, 132.2, 139.0, 153.1, 163.2, 165.1, 188.8 (ArC═O). IR (KBr): ν (cm^{-1}) 968, 1252, 1598, 1658, 2929. MALDI-TOF m/z: 1491.44 $[M+Na]^+$.

Cavitand ***7a***. White solid, 55% (190 mg). mp. 218−220 °C. Anal. Calcd for $C_{100}H_{124}N_4O_{16}$: C, 73.32; H, 7.63; N, 3.42. Found: C, 73.59; H, 7.64; N, 3.40. ^{1}H NMR (500 MHz, DMSO-d_6): δ 0.84 (t, J = 7.0 Hz, 12H, CH_2CH_3), 1.19−1.32 (br m, 40H, $(CH_2)_5$), 1.50 (quint, J = 7.0 Hz, 8H, $CH_2CH_2CH_2)_5$), 1.90 (d, J = 7.3 Hz, 12H, CH_3CH), 3.22 (q, J = 6.4 Hz, 8H, NH−CH_2CH_2), 4.49 (d, J = 7.4 Hz, 4H, inner of OCH_2O), 4.85−4.94 (br s, 12H, $ArCH_2O$ overlapping with CH_3CH), 5.79 (d, J = 7.4 Hz, 4H, outer of OCH_2O), 6.95 (d, J = 8.6 Hz, 8H, Ar), 7.77 (d, J = 8.6 Hz, 8H, Ar), 7.92 (s, 4H, Ar), 8.26 (t, J = 5.5 Hz, 4H, N−H). ^{13}C {^{1}H} NMR (125 MHz, DMSO-d_6): δ 13.8, 16.0, 22.0, 26.5, 28.6, 28.7, 29.1, 31.2, 31.3, 39.1, 60.4, 99.3, 113.9, 122.41, 122.44, 127.3, 128.9, 139.0, 153.1, 160.4, 165.4 (ArC═O). IR (KBr): ν (cm^{-1}) 968, 1250, 1505, 1608, 1635, 2926. MALDI-TOF m/z: 1659.98 $[M+Na]^+$, 1637.89 $[M+H]^+$.

Cavitand ***7b***. White solid, 57% (163 mg). Mp. 191−196 °C. Anal. Calcd for $C_{104}H_{124}N_4O_{20}$: C, 71.37; H, 7.14; N, 3.20. Found: C, 71.62; H, 7.18; N, 3.22. ^{1}H NMR (500 MHz, DMSO-d_6): δ 0.84 (br t, J = 7.0 Hz, 12H, CH_2CH_3), 1.17−1.34 (br m, 40H, $(CH_2)_5$), 1.50 (br s, 8H, $CH_2CH_2CH_2)_5$), 1.90 (d, J = 7.3 Hz, 12H, CH_3CH), 3.20 (br q, J = 6.4 Hz, 8H, NH−CH_2CH_2), 4.47 (br d, J = 7.4 Hz, 4H, inner of OCH_2O), 4.85−4.99 (br s, 12H, $ArCH_2O$ overlapping with CH_3CH), 5.81 (br d, J = 7.4 Hz, 4H, outer of OCH_2O), 7.08 (br d, J = 8.4 Hz, 8H, Ar), 7.90−7.96 (br s, 12H, Ar), 8.78 (br s, 4H, N−H). ^{13}C {^{1}H} NMR (125 MHz, DMSO-d_6): δ 13.9, 16.0, 22.0, 26.3, 28.56, 28.57, 28.7, 31.1, 31.3, 38.3, 60.7, 99.4, 114.6, 122.0, 122.7, 126.0, 132.2, 139.0, 153.1, 163.2, 165.0 (N(H)C═O), 188.7 (ArC═O). IR (KBr): ν (cm^{-1}) 969, 1169, 1252, 1598, 1658, 2927. MALDI-TOF m/z: 1771.54 $[M+Na]^+$.

Cavitand ***8a***. White solid, 52% (155 mg). Mp. > 195 °C (dec.). Anal. Calcd for $C_{84}H_{92}N_4O_{16}$: C, 71.37; H, 6.56; N, 3.96. Found: C, 71.58; H, 6.53, N, 3.98. ^{1}H NMR (500 MHz, DMSO-d_6): δ 1.36 (s, 36H, $C(CH_3)_3$), 1.90 (d, J = 7.3 Hz, 12H, CH_3CH), 4.49 (d, J = 7.4 Hz, 4H, inner of OCH_2O), 4.83−4.93 (br s, 12H, $ArCH_2O$ overlapping with CH_3CH), 5.79 (d, J = 7.4 Hz, 4H, outer of OCH_2O), 6.93 (d, J = 8.7 Hz, 8H, Ar), 7.53 (s, 4H, N−H), 7.74 (d, J = 8.7 Hz, 8H, Ar), 7.91 (s, 4H, Ar). ^{13}C {^{1}H} NMR (125 MHz, DMSO-d_6): δ 16.0, 28.6, 31.2, 50.6, 60.5, 99.3, 113.7, 122.4, 122.5, 128.4, 129.1, 139.0, 153.0, 160.3, 165.6 (ArC═O). IR (KBr): ν (cm^{-1}) 970, 1240, 1500, 1606, 1655, 2970. MALDI-TOF m/z: 1435.49 $[M+Na]^+$.

Cavitand ***9a***. White solid, 39% (124 mg). mp. > 188 °C (dec.). Anal. Calcd for $C_{84}H_{84}N_4O_{24}$: C, 65.79; H, 5.52; N, 3.65. Found: C, 66.10; H, 5.52; N, 3.67. ^{1}H NMR (500 MHz, DMSO-d_6): δ 1.38 (d, J = 7.2 Hz, 12H, $CHCH_3COOMe$), 1.90 (d, J = 7.2 Hz, 12H, CH_3CH), 3.62 (s, 12H, COOC*H*3), 4.41−4.54 (m, 8H, inner of OCH_2O overlapping with $CHCH_3COOMe$), 4.85−4.95 (br s, 12H, $ArCH_2O$ overlapping with CH_3CH), 5.82 (d, J = 7.4 Hz, 4H, outer of OCH_2O), 6.99 (d, J = 8.7 Hz, 8H, Ar), 7.83 (d, J = 8.7 Hz, 8H, Ar), 7.91 (s, 4H, Ar), 8.60 (d, J = 6.7 Hz, 4H, N−H). ^{13}C {^{1}H} NMR (125 MHz, DMSO-d_6): δ 16.0, 16.7, 31.3, 48.1, 51.7, 60.5, 99.3, 114.0, 122.4, 122.5, 126.2, 129.3, 139.0, 153.1, 160.8, 165.6, 173.2. IR (KBr): ν (cm^{-1}) 974, 1249, 1502, 1606, 1653, 1738, 2949. MALDI-TOF m/z: 1555.28 $[M+Na]^+$.

■ ASSOCIATED CONTENT

Supporting Information

The Supporting Information is available free of charge on the ACS Publications website at DOI: 10.1021/acs.joc.6b02472.

The NMR spectra of the reference compounds, those of the products of the Pd-catalyzed self-sorting experiments, the Cartesian coordinates of the optimized geometries, and the obtained thermodynamic quantities (PDF)

■ AUTHOR INFORMATION

Corresponding Author

*zscsok@iqsc.usp.br

ORCID

Rodrigo Q. Albuquerque: 0000-0001-9064-4982

Zsolt Csók: 0000-0001-9432-3879

Notes

The authors declare no competing financial interest.

DOI: 10.1021/acs.joc.6b02472
J. Org. Chem. 2017, 82, 390−396

■ ACKNOWLEDGMENTS

Financial support from Brazilian Agencies CNPq (400112/2014-0), CAPES (A061_2013), FAPESP (2014/02071-5), and the Hungarian Scientific Research Fund (OTKA K113177) are gratefully acknowledged.

■ REFERENCES

(1) Wu, A. X.; Isaacs, L. *J. Am. Chem. Soc.* **2003**, *125*, 4831−4835.
(2) Safont-Sempere, M. M.; Fernández, G.; Würthner, F. *Chem. Rev.* **2011**, *111*, 5784−5814.
(3) Lal Saha, M.; Schmittel, M. *Org. Biomol. Chem.* **2012**, *10*, 4651−4684.
(4) Nelson, D. L.; Cox, M. M *Lehninger Principles of Biochemistry*, 5th ed.; W. H. Freeman and Company: New York, 2008.
(5) Watson, J. D.; Crick, F. H. C. *Nature* **1953**, *171*, 737−738.
(6) Jiang, W.; Winkler, H. D. F.; Schalley, C. A. *J. Am. Chem. Soc.* **2008**, *130*, 13852−13853.
(7) He, Z.; Jiang, W.; Schalley, C. A. *Chem. Soc. Rev.* **2015**, *44*, 779−789.
(8) Jolliffe, K. A.; Timmerman, P.; Reinhoudt, D. N. *Angew. Chem., Int. Ed.* **1999**, *38*, 933−937.
(9) Braekers, D.; Peters, C.; Bogdan, A.; Rudzevich, Y.; Böhmer, V.; Desreux, J. F. *J. Org. Chem.* **2008**, *73*, 701−706.
(10) Rudzevich, Y.; Rudzevich, V.; Klautzsch, F.; Schalley, C. A.; Böhmer, V. *Angew. Chem., Int. Ed.* **2009**, *48*, 3867−3871.
(11) Ajami, D.; Schramm, M. P.; Volonterio, A.; Rebek, J., Jr. *Angew. Chem., Int. Ed.* **2007**, *46*, 242−244.
(12) Ajami, D.; Hou, J.-L.; Dale, T. J.; Barrett, E.; Rebek, J., Jr. *Proc. Natl. Acad. Sci. U. S. A.* **2009**, *106*, 10430−10434.
(13) Chas, M.; Gil-Ramírez, G.; Ballester, P. *Org. Lett.* **2011**, *13*, 3402−3405.
(14) Pinalli, R.; Cristini, V.; Sottili, V.; Geremia, S.; Campagnolo, M.; Caneschi, A.; Dalcanale, E. *J. Am. Chem. Soc.* **2004**, *126*, 6516−6517.
(15) Kobayashi, K.; Yamada, Y.; Yamanaka, M.; Sei, Y.; Yamaguchi, K. *J. Am. Chem. Soc.* **2004**, *126*, 13896−13897.
(16) Yamanaka, M.; Yamada, Y.; Sei, Y.; Yamaguchi, K.; Kobayashi, K. *J. Am. Chem. Soc.* **2006**, *128*, 1531−1539.
(17) Gan, H.; Gibb, B. C. *Chem. Commun.* **2012**, *48*, 1656−1658.
(18) Jedrzejewska, H.; Wierzbicki, M.; Cmoch, P.; Rissanen, K.; Szumna, A. *Angew. Chem., Int. Ed.* **2014**, *53*, 13760−13764.
(19) Szymanski, M.; Wierzbicki, M.; Gilski, M.; Jedrzejewska, H.; Sztylko, M.; Cmoch, P.; Shkurenko, A.; Jaskólski, M.; Szumna, A. *Chem. - Eur. J.* **2016**, *22*, 3148−3155.
(20) Ma, S.; Rudkevich, D. M.; Rebek, J., Jr. *J. Am. Chem. Soc.* **1998**, *120*, 4977−4981.
(21) Renslo, A. R.; Tucci, F. C.; Rudkevich, D. M.; Rebek, J., Jr. *J. Am. Chem. Soc.* **2000**, *122*, 4573−4582.
(22) Aakeröy, C. B.; Rajbanshi, A.; Desper, J. *Chem. Commun.* **2011**, *47*, 11411−11413.
(23) Csók, Z.; Kégl, T.; Párkányi, L.; Varga, Á.; Kunsági-Máté, S.; Kollár, L. *Supramol. Chem.* **2011**, *23*, 710−719.
(24) Csók, Z.; Takátsy, A.; Kollár, L. *Tetrahedron* **2012**, *68*, 2657−2661.
(25) Nagymihály, Z.; Kollár, L. *Tetrahedron* **2015**, *71*, 2555−2560.
(26) Park, Y. S.; Paek, K. *Org. Lett.* **2008**, *10*, 4867−4870.
(27) Park, Y. S.; Seo, S.; Kim, E.-H.; Paek, K. *Org. Lett.* **2011**, *13*, 5904−5907.
(28) Czibulya, Z.; Horváth, É.; Nagymihály, Z.; Kollár, L.; Kunsági-Máté, S. *Supramol. Chem.* **2016**, *28*, 582−588.
(29) Arduini, A.; Bussolati, R.; Credi, A.; Secchi, A.; Silvi, S.; Semeraro, M.; Venturi, M. *J. Am. Chem. Soc.* **2013**, *135*, 9924−9930.
(30) Neal, E. A.; Goldup, S. M. *Angew. Chem., Int. Ed.* **2016**, *55*, 12488−12493.
(31) Mukhopadhyay, P.; Zavalij, P. Y.; Isaacs, L. *J. Am. Chem. Soc.* **2006**, *128*, 14093−14102.
(32) Stewart, J. J. P. *J. Mol. Model.* **2007**, *13*, 1173−1213.
(33) Klamt, A.; Schüürmann, G. *J. Chem. Soc., Perkin Trans. 2* **1993**, *2*, 799−805.
(34) Clayden, J.; Greeves, N., Warren, S. *Organic Chemistry*, 2nd ed; Oxford University Press: Oxford, 2012.
(35) (a) Stewart, J. P. *Stewart Computational Chemistry*, Version 15.180 m; Colorado Springs, CO, USA, http://openmopac.net, 2012. (b) Maia, J. D. C.; Carvalho, G. A. U., Jr.; Mangueira, C. P.; Santana, S. R.; Cabral, L. A. F.; Rocha, G. B. *J. Chem. Theory Comput.* **2012**, *8*, 3072−3081.

DOI: 10.1021/acs.joc.6b02472
J. Org. Chem. 2017, 82, 390−396